Title

AUTOMATED GENERATION OF LINKAGE LOOP EQUATIONS FOR PLANAR 1-DOF LINKAGES, DEMONSTRATED UP TO 8-BAR

Journal

PROCEEDINGS OF THE ASME INTERNATIONAL DESIGN ENGINEERING TECHNICAL CONFERENCES AND COMPUTERS AND INFORMATION IN ENGINEERING CONFERENCE, 2014, VOL 5A, 7(1)

ISSN

1942-4302

ISBN

978-0-7918-4636-0

Authors

Parrish, Brian E
McCarthy, J Michael
Eppstein, David

Publication Date

2014

DOI

10.1115/1.4029306

Peer reviewed

Proceedings of the ASME 2014 International Design Engineering Technical Conferences & Computers and Information in Engineering Conference
IDETC/CIE 2014
August 17-20, 2014, Buffalo, New York, USA

DETC2014-35263

AUTOMATED GENERATION OF LINKAGE LOOP EQUATIONS FOR PLANAR 1-DOF LINKAGES, DEMONSTRATED UP TO 8-BAR

Brian E. Parrish*
Robotics and Automation Laboratory
Department of Mechanical and Aerospace Engineering
University of California
Irvine, California 92697
Email: bparrish@uci.edu

J. Michael McCarthy
Robotics and Automation Laboratory
Department of Mechanical and Aerospace Engineering
University of California
Irvine, California 92697
Email: jmmccart@uci.edu

David Eppstein
Information and Computer Sciences
Department of Computer Science
University of California
Irvine, California 92697
Email: eppstein@ics.uci.edu

ABSTRACT

In this paper we present an algorithm that automatically creates the linkage loop equations for planar 1-DoF linkages of any topology with rotating joints, demonstrated up to 8-bars. The algorithm derives the linkage loop equations from the linkage graph by establishing a cycle basis through a single common edge. Divergent and convergent loops are identified and used to establish the fixed angles of the ternary and higher links.

Results demonstrate the automated generation of the linkage loop equations for the five distinct 6-bar mechanisms, Watt I-II and Stephenson I-III, as well as the seventy one distinct 8-bar mechanisms.

The resulting loop equations enable the automatic derivation of the Dixon determinant for linkage kinematic analysis of the position of every possible assembly configuration. The loop equations also enable the automatic derivation of the Jacobian for singularity evaluation and tracking of a particular assembly configuration over the desired range of input angles.

The methodology provides the foundation for the automated configuration analysis of every topology and every assembly configuration of 1-DoF linkages with rotating joints up to 8-bar. The methodology also provides a foundation for automated configuration analysis of 10-bar and higher linkages.

*Address all correspondence to this author.

INTRODUCTION

Dimensional synthesis solves for the geometric features of a linkage so that it is capable of moving the end-effector to each of a given set of positional requirements. One type of synthesis, task generation, solves the geometry to meet a set of task positions that are specified by their global positions and angles, Fig. 1. Synthesis, however, does not guarantee that the linkage will move smoothly, continuously with an increasing input angle, through all angles between the task positions.

A kinematic chain is an assembly of rigid bodies, links, connected by joints. The topology of a kinematic chain is the specific interconnection of the links and can be represented by either an adjacency matrix or an adjacency graph. A mechanism, sometimes called an inversion, is a kinematic chain of a specific topology where a link has been selected as ground. A linkage is a mechanism with a particular link selected as the input link, therefore, a linkage is a specific topology of a kinematic chain where one link is selected as ground and another link is selected as the input. The scope of this paper is limited to input links that are adjacent to, connected to, ground.

The motivation for this paper is to automate the complete configuration analysis of a synthesized linkage to ensure continuous smooth movement through all input angles within the range of interest. In this paper we present the first key step, an algorithm that automatically constructs the linkage loop equations for any topology of planar 1-DoF linkage with rotating joints up to

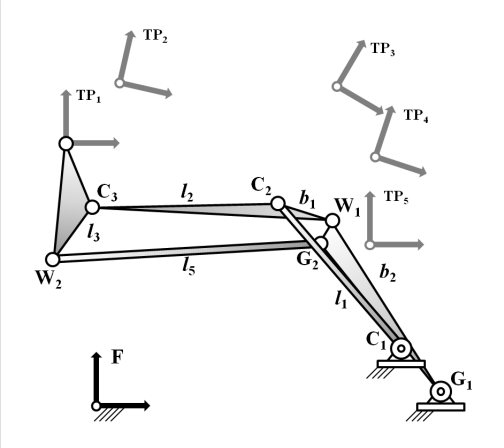

FIGURE 1: EXAMPLE WATT I LINKAGE REACHING A TASK POSITION.

8-bars.

To complete the automation of the configuration analysis the Dixon determinant can be derived from the loop equations and used to solve for all possible assembly configurations. Continuous smooth movement can be determined from the linkage loop equations by deriving and solving the Jacobian to identify singularities for the configuration of interest within the range of desired input angles. The form of the automatically constructed linkage loop equations is sufficient for automated derivation of both the Dixon determinant and the Jacobian but the details of that automation are beyond the scope of this paper.

This algorithm has been verified on all 4, 6 and 8-bar topologies for all unique combinations of the ground link and the ground-connected input link. The approach is general therefore it also forms a basis for automating the analysis of 1-DoF kinematic chains of higher link counts.

LITERATURE REVIEW

The specific connectivity of a kinematic chain can be represented as an adjacency graph where the vertices represent links and the edges represent joints between the links. Tsai [1] published an atlas of the sixteen 1-DoF 8-bar, 10-joint kinematic chains and represented them in a set of linkage adjacency graphs and linkage sketches. A non-planar adjacency graph and a sketch of the Double-Butterfly eight-bar linkage are shown in Fig. 2.

Much of the work today is enumerating the unique kinematic chains with high link counts. A key component of the enumeration process is the detection and elimination of isomorphic kinematic chains. Isomorphic kinematic chains are not unique because they have topologies that can be transformed into a topology that has already been enumerated by simply renumbering

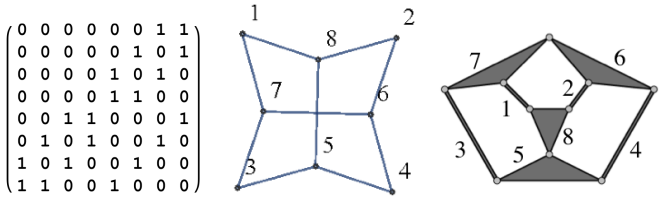

FIGURE 2: DOUBLE BUTTERFLY 8-BAR ADJACENCY MATRIX, GRAPH AND LINKAGE SKETCH

the vertices. Sunkari and Schmidt [2] apply a McKay-type algorithm [3] to show that there are approximately 20 million non-isomorphic topologies for the 16 bar, 22 joint, kinematic chain. Ding and Huang [4] established a canonical representation of the linkage graphs and published a method for isomorphism detection based on the largest perimeter loop and the degrees of the vertices. Ding et al. [5] published the enumeration of graphs of kinematic chains up to 14-bars and recently published work extending the development of linkage graphs to linkages that contain multiple joints, joints on a common axis [6].

Tuttle [7] determined the number of distinct inversions, mechanisms, of the 1, 2 and 3-DoF kinematic chains. The results show that for 1-DoF linkages there are five distinct 6-bar mechanisms and 71 distinct 8-bar mechanisms.

Using Baranov trusses Manolescu [8] identifies the three distinct Stephenson 6-bar mechanisms and the two distinct Watt 6-bar mechanisms, total of five, as well as 19 unique linkages. Of those 19 unique linkages nine have a ground-connected input. Verho [9] allows actuation through link pairs that are not grounded and identifies 25 unique six-bar linkages using Assur groups and visual inspection. Of those 25 linkages nine have a ground-connected input and match the nine identified by Manolescu.

Linkage synthesis solves for the specific dimensions of the links using one of the enumerated topologies. Soh and McCarthy [10] published a methodology specific to the 8-bar family for synthesizing linkages that can be constructed from a pair of constrained 3-R chains. Linkage synthesis approaches are published for a variety of linkage topologies [11–13] but since all possible topologies of 1-DoF linkages with rotating joints are known for the 8-bar family, every synthesized linkage must be in one of these topologies.

Linkage configuration analysis solves for the angles of all of the output links. Approaches are typically shown for specific topologies. For example, the graph shown in Fig. 2 represents a Double Butterfly 8-bar linkage. Wampler [14] referencing Dixon [15] analyzed a Double Butterfly linkage using the Dixon determinant in a complex plane formulation. The same linkage was also evaluated in rational formulation by Nielsen and Roth [16]. Various other methods for solving the configuration

of a linkage have been published such as the Gröbner-Sylvester method by Dhingra et al. [17] and the linear relaxation method by Porta et al. [18].

To determine if a particular assembly configuration is usable the singular configurations must be avoided. Linkages that encounter a singularity within the range of motion of interest have a branching defect. Several authors address the singularities of linkages. Chase and Mirth [19] use the sign of the determinant of the Jacobian to identify the branches of six-bar linkages. Myszka et al. [20] identifies the singularities and plots the singular configurations as curves that are a function of the length of one of the links.

Kecskeméthy et al. [21] published work automating the generation of the equations of motion of multibody systems. The method establishes a minimal cycle basis for the mechanism graph, generates local dynamics solutions for each mechanism loop, and then combines the local dynamics solutions into a global solution.

A general method for automating configuration analysis for all topologies of planar 1 DoF linkages has not been published.

Demonstrated up to the 8-bar family our contribution shows a method to automatically produce the linkage loop equations for any 1-DoF linkage with rotary joints. The loop equations are in a form sufficient to complete the automation of the configuration analysis by enabling automated derivation of the Dixon determinant and the Jacobian.

LINKAGE GRAPH AND ADJACENCY MATRIX

The number of joints in a planar 1-DoF linkage is given as a function of the number of links by the equation

$$j = 3n/2 - 2 \tag{1}$$

The number of linkage loops is given by

$$L = j - n + 1 \tag{2}$$

Beginning with the 4-bar kinematic chain, the planar 1-DoF kinematic chains are comprised of loops of links. The 8-bar 1-DoF kinematic chains exist in three link assortment families. The link assortment is the quantity of links in the kinematic chain that connect to 2, 3, 4, 5, etc. adjacent links. The links are called binary, ternary, quaternary, quintenary, etc. The planar one-DoF link assortments and the quantity of topologies for each are listed in Table 1 up to 8-bars, Tsai [1].

Each topology can be represented in the form of an adjacency matrix where a "1" indicates a connection between vertices and a "0" indicates no connection between the two vertices. For planar 1-DoF linkages, the number of connections between two links is limited to one since a revolute joint only allows 1-DoF. Having two joints between links forms a rigid structure. For the Double Butterfly linkage the adjacency matrix and adjacency graph are shown in Fig. 2.

TABLE 1: PLANAR 1-DOF KINEMATIC CHAIN TOPOLOGIES

Class			Link Assortment				Topology	
Loops	n	j	n_2	n_3	n_4	n_5	Quantity	Total
1	4	4	4	0	0	0	1	1
2	6	7	4	2	0	0	2	2
3	8	10	4	4	0	0	9	16
			5	2	1	0	5	
			6	0	2	0	2	

DERIVING THE LINKAGE LOOPS

The process to automatically construct the linkage loops for a particular linkage begins with the adjacency graph and the user defined selection for the ground link and ground-connected input link. The first step is to establish the smallest cycle basis for the linkage through a common edge, the edge connecting the ground vertex to the input vertex.

The planar 1-DoF linkages are in the family of graphs called 2-vertex connected. To divide the graph into two separate graphs two vertices must be removed. Removing one vertex leaves a connected graph. This graph property enables the automation of the linkage loop equations.

2-vertex connected graphs have the property that the graph can be decomposed into a set of ears, an ear decomposition. Per Whitney [22] any non-separable graph based on a loop, or circuit, remains a non-separable graph with the addition of ears, also called "suspended chains". For an ear decomposition applied to linkage graphs the first ear is a loop, or cycle. The second ear, and higher, are simple paths that have only the end joints in common with a previous loop or loops. An independent loop can be obtained by following the ear and the previous loop or loops to a common vertex.

A set of independent loops for a graph is called a cycle basis. Our system needs every loop of the basis to pass through the edge connecting the grounded vertex to the input vertex. By using ear decompositions we can show that a basis with this property always exists.

To find this basis we do not find the ears directly, rather we find the loops directly. The list of links along a loop from the input vertex to the ground vertex is called a path and the length of

the path is its number of links. We use a shortest path algorithm to find loops that are of minimal length.

There are several means of identifying the shortest path between two vertices. Because all of the edges in these graphs represent joints they all have a positive distance therefore Dijkstra's shortest path algorithm [23] is sufficient for finding the shortest distance between two vertices. Mathematica has a built-in shortest path function that can be constrained to use the Dijkstra algorithm but the default settings are also suitable.

The shortest paths can be visualized in levels. To generate the loops the list of edges are produced for the entire graph and the edge directly connecting the ground vertex to the input vertex is eliminated. Through the remaining portion of the linkage the shortest path back to ground is identified. This path is the first level. To find the next level of paths an edge in the first level path is eliminated along with the one edge elimination that created that first path, the edge connecting ground and input. All edges in the first level path are eliminated one at a time to produce the second level of paths. To find the third level of paths an edge in a second level path is eliminated along with all the edge eliminations that created that second level path. This process continues until no new paths are found and every edge elimination has been attempted.

At any of these levels, if there are multiple paths of equal length one of them may be selected arbitrarily. At the next level the path not selected will still be the shortest path, therefore it will not be overlooked.

Because these are 2-vertex connected graphs, elimination of two edges can separate the graph into two components such that there are no paths from the input vertex back to ground. When this occurs the elimination is not valid and the algorithm tests the elimination of the next candidate set of edges.

From all of the paths identified, all of the unique paths are collected and formed into cycles by appending the edge between ground and input. The direction along each cycle is consistently defined such that the first vertex in each cycle is ground, the second vertex is input, and the last vertex is ground.

Some of the cycles may not be independent. An independent cycle will contain an edge that is not in any of the previous cycles. The cycles are ordered by length and then by vertex degree along the cycles. The smallest independent cycle set that contains every edge of the graph is chosen as the cycle basis through a common edge, the edge connecting ground to input.

EXAMPLE AUTOMATED LOOP DERIVATION

We apply the automation to an example 8-bar linkage from one the nine topologies in the 4400 link assortment group. The adjacency graph and adjacency matrix for is shown in Fig. 3. Vertex five is the selected ground link and vertex 2 is the selected input link.

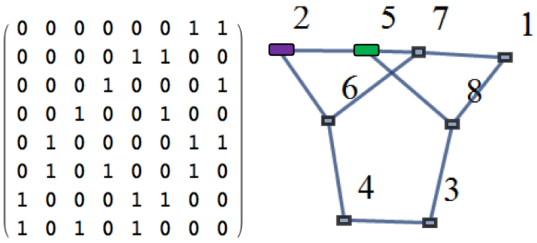

FIGURE 3: EXAMPLE EIGHT BAR ADJACENCY MATRIX AND ADJACENCY GRAPH

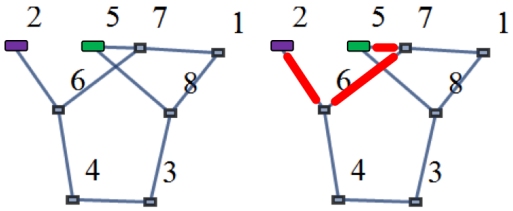

FIGURE 4: IDENTIFYING THE FIRST SHORTEST PATH

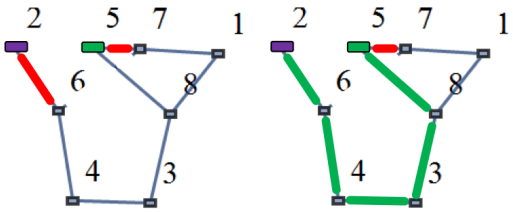

FIGURE 5: IDENTIFYING THE SECOND SHORTEST PATH

The first elimination is the edge connecting ground to input, (5–2), and the first level shortest path for the example 8-bar is shown in Fig. 4

To find the shortest paths at the second level each of the edges along the first shortest path is eliminated one at a time along with the edge connecting ground to input. The next shortest path back to ground is found through the rest of the linkage. Elimination of the edge set (5–2) and (2–6) will eliminate all connections to the input vertex, therefore the first valid edge elimination set is (5–2) and (6–7), Fig. 5.

To find the third level paths, an edge in each of the second level paths is eliminated along with the edge eliminations that formed the second level path. The first valid elimination set is the edges (5–2), (6–7), and (8–5). This elimination produces the shortest path shown in Fig. 6.

The last unique third level path is found by eliminating the edge set (5–2), (7–5), and (6–4). This elimination produces the

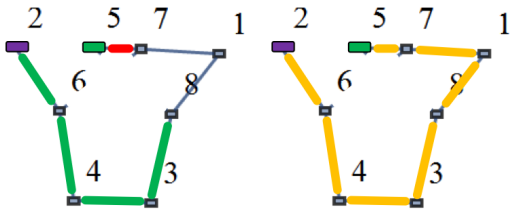

FIGURE 6: IDENTIFYING THE THIRD SHORTEST PATH

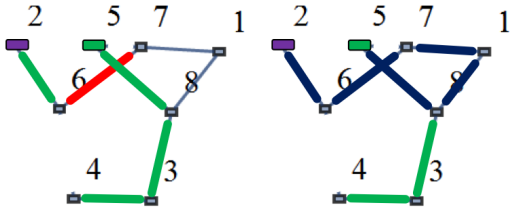

FIGURE 7: IDENTIFYING THE FOURTH SHORTEST PATH

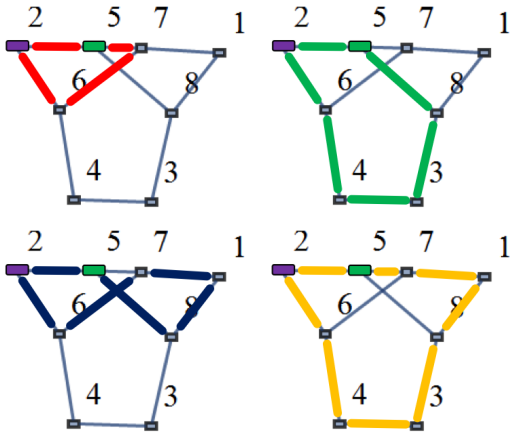

FIGURE 8: THE FOUR UNIQUE CYCLES

shortest path shown in Fig. 7.

The unique shortest paths are formed into cycles by adding the edge connecting ground and input. The four unique cycles are sorted by length and loop vertex degree and shown in Fig. 8.

The cycle basis is the first three cycles. The loops and the vertex degrees are shown in Table. 2.

UNIQUE MECHANISMS AND UNIQUE LINKAGES

The automation must be able to analyze the configuration of all unique linkages, specifically, all unique combinations of topology, ground link and ground-connected input link. To test the analysis routine we enumerated and analyzed all of the unique linkages.

TABLE 2: EXAMPLE LINKAGE CYCLE BASIS AND VERTEX DEGREE LIST

Loop	Cycle Basis	Vertex Degree List
1	{5,2,6,7,5}	{3,2,3,3,3}
2	{5,2,6,4,3,8,5}	{3,2,3,2,2,3,3}
3	{5,2,6,7,1,8,5}	{3,2,3,3,2,3,3}

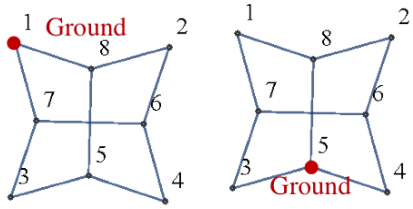

FIGURE 9: DOUBLE BUTTERFLY UNIQUE MECHANISMS

For each linkage there may be several choices for the ground link that produce the same mechanism. Similar to the definition of a graph isomorphism the same mechanism will have a graph with a one-to-one correspondence of vertices that preserve the incidence as well as the correspondence of the selected ground link. For example, the Double Butterfly 8-bar mechanism has only two choices for the ground vertex that are unique, Fig. 9. Every other selection for the ground vertex can be made into one of these two forms by renumbering the vertices.

Several selections of ground and ground-connected input link may produce the same linkage. Similar to a graph isomorphism and a non-unique mechanism, the graph of a non-unique linkage will have a one-to-one correspondence of vertices that preserve the incidence as well as the correspondence of the selected ground link and input link. For the Double Butterfly 8-bar linkage there are only three choices for the ground and ground-connected input vertex that are unique, Fig. 10. Every other selection for the ground and ground-connected input vertices can be made into one of these three forms by renumbering the vertices.

To identify a non-unique linkage the algorithm compares the incidence of the vertices along the cycles of the smallest cycle basis through the common edge connecting ground and input. The two cycle bases being compared have both been consistently sorted by cycle length and consistently ordered within each cycle such that the first vertex is ground, the second vertex is the ground-connected input, and the last vertex is ground. The incidence of each cycle is represented by the vertex degrees taken in order along the loop. Eight-bar linkages that are not unique pre-

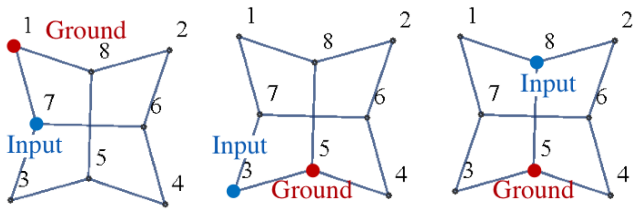

FIGURE 10: DOUBLE BUTTERFLY UNIQUE LINKAGES

serve the incidence along the loops of the cycle basis, meaning, they have the same set of three vertex degree lists in the same order. Defined by the ground-input common edge cycle basis every 8-bar has a unique set of three vertex degree lists.

DEFINING THE LINKAGE DIMENSIONAL FEATURES

To automatically establish the linkage loop equations we apply a naming convention to the linkage loops to construct unique names for the links, the joints, and the lines between joints along a loop. We also define the name and location of the link angles and the fixed angles representing divergence and convergence of loops on ternary and higher links. When two loops diverge or converge we only name the lines along the two loops and the angle between them. This provides a complete geometric description of the triangle formed by the three joints. The only input needed to construct the loop equations is the cycle basis.

The cycle basis provides an ordered list of vertices for each loop. These vertices are also the names of the linkage links which are joined in order along each loop. Following the cycle basis along each loop we assign a unique name for the joints based on the links being joined. Because there is only one joint between any two links these joint names are always unique. The first character of the joint name is "j", followed by the number of the first link being joined, followed by "t", and finished with the number of the second link being joined. For example, a joint between link 1 and link 5 is called $j1t5$. The "t" enables unambiguous distinction between links even when the link number is more than one digit.

Also following the order of the links as shown for each linkage loop, the distance between two joints on the same link is given a unique name based on the two end joints. The first character is "L", followed by the name of the first joint (with the "j" omitted), followed by "t", followed by the last digits of the ending joint. For example, the dimension of the line on link 5 between the joints $j1t5$ and $j5t2$ is called $L1t5t2$. In a binary link this dimension is intuitive, the distance between the two joints. In a ternary link, this is the distance between two of the three joints.

For evaluating angles we use the convention that all angles are positive counter clockwise. The global angle of a link is defined from a global reference to a feature on the link. The selected global reference is the x axis. The selected feature on a binary link is intuitive, the line between the two joints. For ternary and higher links there will be two or more features that could be selected. We define the global angle of the link as the angle from the global x axis to the line between the joints along the first loop that contains the link. The origin of that angle is the first joint of the link encountered along the loop. The name assigned to this angle is "th" followed by the link number. For example if dimension $L1t5t2$ is part of the first loop then the angle relative to the global frame for $L1t5t2$ is called $th5$ and the origin of that angle is at the joint $j1t5$.

The vertices where the loops diverge (or converge) represent ternary or higher links. We need to define the angle for the line along the divergent or convergent loop. We do this by defining a fixed angle to describe the angle of the divergent (or convergent) loop relative to the reference loop from which loop diverges (or converges). This fixed angle is added to the angle defining the line along the reference loop. The fixed angle is located at the common joint and begins from the line along the reference loop and ends at the line along the divergent (or convergent) loop. The name of the fixed angle is based on the two lines. The name is "fix" followed by the name of the line in the reference loop (with the "L" omitted), followed by "tt", followed by the name of the line along the divergent (or convergent) loop (with the "L" omitted). In quaternary links there will be three loops that pass through the link. The third loop may diverge or converge relative to a line that diverges or converges from the link angle. The same naming convention applies in this case so the final angle of the third loop will be a summation of the link angle and two fixed angles.

We apply the naming convention to an example Stephenson 6-bar linkage in Fig. 11.

CONVERTING CYCLES TO LOOP EQUATIONS

To automate the process of developing the loop equations we apply the naming convention by automating the construction of a convention called FTLA. FTLA describes the line on each link, e.g. $L1t5t2$, that is connected to the next link along each loop with four terms {From Joint, To Joint, Link Dimension, Angle}. Each loop is represented by a series of these four-term sets and the first of the four term sets for each loop represents the line between two joints on the ground link. To sufficiently define a line between two joints only three of these four terms are needed and the fourth can be derived, however, we choose to retain all four terms for convenience. The only input needed to develop the FTLA is the cycle basis.

To create the FTLA for a linkage, first the cycle basis is converted to the series of joints it represents. The joints are then paired to represent the end points of the lines on the links along the linkage loops. The lines between the joints are named based

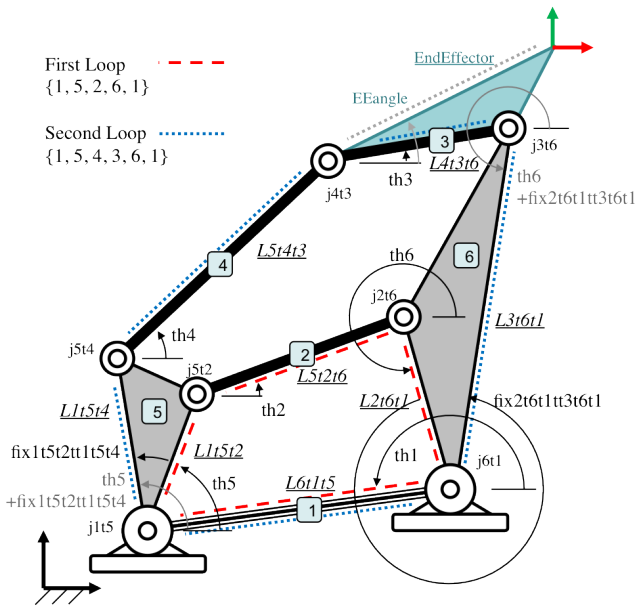

FIGURE 11: NAMING CONVENTION, STEPHENSON 6-BAR

on the joints and ordered such that the first line in each FTLA represents a line on the ground link.

The angle for a given line is defined in two steps. First we establish the global angle from the x axis to the link, specifically to the line between the joints along the first loop that contains the link. Second we establish the fixed angle that must be added to the reference line to properly define the divergent or convergent line. When two loops converge the "To Joint" will match, when two loops diverge the "From Joint" will match. Subtracting the "From Joint" and "To Joint" terms of each previous loop from the same terms in the current loop reveals the locations where the current loop converges or diverges from a previous loop. These fit the form of Eqn. 3.

$$\begin{aligned} &\text{Convergent Loop Form} : \{Joint_2 - Joint_1, 0\}, \\ &\text{Divergent Loop Form} : \{0, Joint_2 - Joint_1\}. \end{aligned} \tag{3}$$

Because we know which entries in the FTLA lists are subtracted, we know the locations of the loop divergences and convergences so we map the fixed angles to the appropriate location in the FTLA and the appropriate name for the fixed angle is added to the angle defining the reference line.

We convert from the FTLA form to the final loop equations by taking the sum along each loop of the product

$$\begin{aligned} X &: (\text{Link Dimension}) * Cos(Angle) \\ Y &: (\text{Link Dimension}) * Sin(Angle) \end{aligned} \tag{4}$$

EXAMPLE, CREATING THE LOOP EQUATIONS

Using the 8-bar shown in Fig. 3 as our example, the first step uses text manipulation of the cycle basis to define the terms {From Joint, To Joint, Link Dimension, Link Angle}. At this first step the link angle does not account for the fixed angles between divergent or convergent loops. The pairs of joints along the loops are shown in Eqn. 5.

$$\begin{aligned} \text{Loop 1} &: \{j7t5, j5t2\}, \{j5t2, j2t6\}, \{j2t6, j6t7\}, \{j6t7, j7t5\} \\ \text{Loop 2} &: \{j8t5, j5t2\}, \{j5t2, j2t6\}, \{j2t6, j6t4\}, \{j6t4, j4t3\}, \\ &\quad \{j4t3, j3t8\}, \{j3t8, j8t5\} \\ \text{Loop 3} &: \{j8t5, j5t2\}, \{j5t2, j2t6\}, \{j2t6, j6t7\}, \{j6t7, j7t1\}, \\ &\quad \{j7t1, j1t8\}, \{j1t8, j8t5\} \end{aligned} \tag{5}$$

Using Eqn. 5 we subtract each term in Loop 1 from each term in Loop 2 to reveal where the loops diverge and converge. Loop 2 and Loop 1 converge at $j5t2$ and diverge at $j2t6$. The difference between the two loops fit the desired pattern at these joints, Eqn. 6.

$$\begin{aligned} \{j8t5, j5t2\} - \{j7t5, j5t2\} &= \{j8t5 - j7t5, 0\} \\ \{j2t6, j6t4\} - \{j2t6, j6t7\} &= \{0, j6t4 - j6t7\}. \end{aligned} \tag{6}$$

The same process is applied to Loop 3 relative to Loop 1 and Loop 2. Loop 3 converges to Loop 1 at $j5t2$ following the same path along $L8t5t2$ as Loop 2 therefore the fixed angle about $j5t2$ is the same for both Loop 2 and Loop 3. Loop 3 also converges to Loop 2 at $j8t5$ and diverges from Loop 1 at $j6t7$.

The locations of the loop divergences and convergences are mapped to the appropriate location in the loops and the appropriate name for the fixed angle is assigned. The final angle of the linkage feature is the sum of the fixed angle and the link angle.

The final FTLA convention is shown in Eqn. 7.

$$
\begin{aligned}
&\text{Loop 1}\{j7t5, j5t2, L7t5t2, th5\}, \{j5t2, j2t6, L5t2t6, th2\},\\
&\qquad \{j2t6, j6t7, L2t6t7, th6\}, \{j6t7, j7t5, L6t7t5, th7\}\\
&\text{Loop 2}\{j8t5, j5t2, L8t5t2, fix7t5t2tt8t5t2 + th5\},\\
&\qquad \{j5t2, j2t6, L5t2t6, th2\},\\
&\qquad \{j2t6, j6t4, L2t6t4, fix2t6t7tt2t6t4 + th6\},\\
&\qquad \{j6t4, j4t3, L6t4t3, th4\}, \{j4t3, j3t8, L4t3t8, th3\},\\
&\qquad \{j3t8, j8t5, L3t8t5, th8\}\\
&\text{Loop 3}\{j8t5, j5t2, L8t5t2, fix7t5t2tt8t5t2 + th5\},\\
&\qquad \{j5t2, j2t6, L5t2t6, th2\}, \{j2t6, j6t7, L2t6t7, th6\},\\
&\qquad \{j6t7, j7t1, L6t7t1, fix6t7t5tt6t7t1 + th7\},\\
&\qquad \{j7t1, j1t8, L7t1t8, th1\},\\
&\qquad \{j1t8, j8t5, L1t8t5, fix3t8t5tt1t8t5 + th8\} \qquad (7)
\end{aligned}
$$

The final loop equations are shown in Eqn. 8.

$$
\begin{aligned}
&\text{Loop 1}\\
&\quad X : L5t2t6\cos(th2) + L7t5t2\cos(th5)\\
&\qquad + L2t6t7\cos(th6) + L6t7t5\cos(th7) = 0\\
&\quad Y : L5t2t6\sin(th2) + L7t5t2\sin(th5)\\
&\qquad + L2t6t7\sin(th6) + L6t7t5\sin(th7) = 0\\
&\text{Loop 2}\\
&\quad X : L5t2t6\cos(th2) + L4t3t8\cos(th3)\\
&\qquad + L6t4t3\cos(th4) + L8t5t2\cos(fix7t5t2tt8t5t2 + th5)\\
&\qquad + L2t6t4\cos(fix2t6t7tt2t6t4 + th6)\\
&\qquad + L3t8t5\cos(th8) = 0\\
&\quad Y : L5t2t6\sin(th2) + L4t3t8\sin(th3)\\
&\qquad + L6t4t3\sin(th4) + L8t5t2\sin(fix7t5t2tt8t5t2 + th5)\\
&\qquad + L2t6t4\sin(fix2t6t7tt2t6t4 + th6)\\
&\qquad + L3t8t5\sin(th8) = 0\\
&\text{Loop 3}\\
&\quad X : L7t1t8\cos(th1) + L5t2t6\cos(th2)\\
&\qquad + L8t5t2\cos(fix7t5t2tt8t5t2 + th5) + L2t6t7\cos(th6)\\
&\qquad + L6t7t1\cos(fix6t7t5tt6t7t1 + th7)\\
&\qquad + L1t8t5\cos(fix3t8t5tt1t8t5 + th8) = 0\\
&\quad Y : L7t1t8\sin(th1) + L5t2t6\sin(th2)\\
&\qquad + L8t5t2\sin(fix7t5t2tt8t5t2 + th5) + L2t6t7\sin(th6)\\
&\qquad + L6t7t1\sin(fix6t7t5tt6t7t1 + th7)\\
&\qquad + L1t8t5\sin(fix3t8t5tt1t8t5 + th8) = 0 \qquad (8)
\end{aligned}
$$

DIXON DETERMINANT DERIVATION

To solve for the angles of all of the links we solve the Dixon determinant using the complex plane formulation as shown by Wampler [14]. To convert the loop equations to complex form we treat the Y direction as along the imaginary plane. Multiply the Y equations by i where $i^2 = -1$ and sum the X and Y equations. We apply trigonometric identities and exponential identities to transform the loop equations into imaginary form. To solve for the unknown link angles the conjugates of the complex loop equations are used to provide the full equation set.

The Dixon determinant method requires the selection of one unknown angle to be used as a generalized eigenvalue while the remaining angles are solved as a generalized eigenvector. The Dixon determinant form is

$$[M\Theta_n - N]\,\mathbf{t} = 0, \qquad (9)$$

where M and N are matrices with constant coefficients comprised of the linkage dimensions, the ground angle, the input angle and the complex conjugate of the input angle. θ_n is the unknown angle selected to be the eigenvalue and the vector $\mathbf{t}$ is the set of monomials representing the remaining unknown link angles.

Some unknown angles are poor choices for the eigenvalue θ_n because the resulting eigenvector $\mathbf{t}$ cannot be used to solve for all of the remaining link angles. To cancel any scaling factors that may exist, the final step of the solution process takes the ratio of two elements of $\mathbf{t}$ to determine the true numerical value of each angle. With a poor selection of θ_n there is no combination of elements in $\mathbf{t}$ whose ratio defines one or more of the unknown angles. To automate this aspect of the procedure we simply test each unknown angle as a candidate eigenvalue, derive the eigenvector $\mathbf{t}$ and verify, symbolically, that there exists a monomial ratio that will produce every unknown angle. The first candidate θ_n that meets this criteria is selected as the eigenvalue.

Some linkages cannot be solved as a whole linkage using the Dixon determinant process, not because of a flaw in the process but because there is no valid selection of the eigenvalue Θ_n. These linkages partition and should be able to be solved as independent sub-linkages.

When a valid eliminant is found, numerical values for the link features are determined from the linkage synthesis and the Dixon determinant is numerically solved for a given input angle. The output provides all of the possible linkage assembly configurations for that input angle.

BLOCK DIAGONAL JACOBIAN DERIVATION

Because the Dixon determinant provides all of the possible real assembly configurations a means of identifying a particular assembly configuration within the solutions is needed. McCarthy

$$\begin{bmatrix} A & B \\ C & D \end{bmatrix} \begin{bmatrix} I & 0 \\ -D^{-1}C & I \end{bmatrix} = \begin{bmatrix} A - BD^{-1}C & B \\ 0 & D \end{bmatrix}$$

FIGURE 12: DETERMINANT PRESERVING TRANSFORM

and Soh [13] show a numerical method to track a particular solution through the range of input angles. The present research identifies a particular linkage assembly by the sign of the determinant of the Jacobian of each loop. The Jacobian is the derivative of each of the six loop equations, Eqn. 8, with respect to each unknown angle. We convert the Jacobian to block upper triangular form through a determinant preserving transform as shown by Silvester [24], Fig. 12. This factors the determinant of the Jacobian into the determinant of the individual 2x2 block matrices along the diagonal.

Since the transform involves an inverse of sub-matrix D the columns of the Jacobian are first sorted so that the blocks along the diagonal are full rank to ensure that D is full rank. For the 8-bar family the Jacobian is a 6x6 matrix and we apply the transform twice, the first transform treats the last 2x2 along the diagonal as D, the second transform treats the middle 2x2 as D.

The example linkage, Fig. 3, has the input link and the ground link within a 4-bar sub-linkage therefore singularities should occur when the following features are collinear: $L2t6t7$ and $L6t7t5$, $L6t4t3$ and $L4t3t8$, or $L7t1t8$ and $L1t8t5$. Taking the determinant of each 2x2 block along the diagonal produces the three Jacobian factors expected, Eqn. 10. One of these factors is zero when one of the expected link pairs is collinear.

$$\begin{aligned} J_1 &: -L2t6t7\ L6t7t5(\cos(th7)\sin(th6) - \cos(th6)\sin(th7)) \\ J_2 &: -L4t3t8\ L6t4t3(\cos(th4)\sin(th3) - \cos(th3)\sin(th4)) \\ J_3 &: -L1t8t5\ L7t1t8(\cos(fix3t8t5tt1t8t5 + th8)\sin(th1) \\ &\quad - \cos(th1)\sin(fix3t8t5tt1t8t5 + th8)). \end{aligned} \tag{10}$$

For many linkages the sign combination of the Jacobian factors uniquely identifies the configuration of interest among the solutions of the Dixon determinant. However, there may be exceptions such as the Stephenson III 6-bar linkage that could contain a link that rotates more than 360 degrees before encountering a singularity [19]. For such linkages the factored Jacobian alone may not be sufficient.

RESULTS

Following this procedure we have automatically derived loop equations for the entire family of 4-bar, 6-bar, and 8-bar 1-DoF linkages with rotating joints. Four 10-bar linkages have also been successfully automated including two with non-planar graphs and one with a quintenary link.

TABLE 3: COUNT OF UNIQUE MECHANISMS AND LINKAGES, 6-BAR AND 8-BAR

Links	Assort.	Topologies	Mechanisms	Linkages
6	4200	2	5	9
8	4400	9	35	76
	5210	5	31	68
	6020	2	5	9
	Total	16	71	153

The quantity of unique linkages identified by this process, Table 3, matches published results. The process identified the five unique six-bar mechanisms, Watt I-II and Stephenson I-III, as well as the nine unique six-bar linkages with a ground connected input, matching the known Watt and Stephenson families. The quantity of 71 unique mechanisms for the eight-bar family matches the result published by Tuttle [7]. The process also provided a new result showing 153 unique eight-bar linkages with a ground-connected input.

The algorithm also identified the Watt IIb linkage uniquely as the one six-bar linkage that partitions. Like the Watt IIb, the algorithm identified 24 linkages in the 8-bar family that do not have an acceptable selection for the eigenvalue angle Θ_n and cannot be solved as a whole linkage using the Dixon determinant. Inspection of these 24 linkages, and the Watt IIb, shows that the ground and input links are driving two one-DoF sub-linkages whose assembly configurations are independent.

CONCLUSIONS

In this paper we present a procedure to automatically create the linkage loop equations for the entire family of 1-DoF linkages with rotating joints up to 8-bars. The process provides equations in a format suitable for automation of the complete configuration analysis for any topology, ground selection, and ground-connected input selection of planar 1-DoF 8-bar linkages. The method is also general and forms the basis for automation of 10-bar and higher linkages.

Extensions of the work are expected to include planar multi-degree of freedom linkages, 10 bar and higher linkages, prismatic joints, inputs not connected to ground, and spherical linkages. We also expect to incorporate improvements in the algorithm for computational efficiency.

ACKNOWLEDGMENT

This material is based upon work supported by the National Science Foundation under Grant No. 1217322 and 1066082 and by the Office of Naval Research under grant N00014-08-1-1015.

REFERENCES

[1] Tsai L.: Mechanism Design: Enumeration of Kinematic Structures According to Function. CRC press. (2000)

[2] Sunkari R. P. and Schmidt L. C.: Structural synthesis of planar kinematic chains by adapting a McKay-type algorithm. Mechanism and Machine Theory, Volume 41, Issue 9, September 2006, pp.1021-1030

[3] McKay B. D.: Isomorph-free exhaustive generation. Journal of Algorithms, Volume 26(2), pp.306-324, 1998

[4] Ding H. and Huang Z.: The Establishment of the Canonical Perimeter Topological Graph of Kinematic Chains and Isomorphism Identification. ASME Journal of Mechanical Design, 129(9), pp.915-923, June (2007)

[5] Ding H., Hou F., Kecskeméthy A., Huang Z.: Synthesis of the whole family of planar 1-DOF kinematic chains and creation of their atlas database. Mechanism and Machine Theory, Volume 47, January 2012, pp.1-15

[6] Ding H., Yang W. Huang P., Kecskeméthy A.: Automatic Structural Synthesis of Planar Multiple Joint Kinematic Chains. ASME Journal of Mechanical Design, 135(9), 091007 (2013) (12 pages)

[7] Tuttle E. R.: Generation of planar kinematic chains. Mechanism and Machine Theory, Volume 31, Issue 6, August 1996, pp.729-748

[8] Manolescu, N. I.: A method based on Baranov trusses, and using graph theory to find the set of planar jointed kinematic chains and mechanisms. Mechanism and Machine Theory, Volume 8, Issue 1, pp.3-22, 1973

[9] Verho, A.: An extension of the concept of the group. Mechanism and Machine Theory, Volume 8, Issue 2, pp.249-256, 1973

[10] Soh G. S. and McCarthy J. M.: Synthesis of Eight-Bar Linkages as Mechanically Constrained Parallel Robots. 12th IFToMM world congress A. Vol. 653. 2007

[11] Perez A. and McCarthy J. M.: Clifford Algebra Exponentials and Planar Linkage Synthesis Equations. ASME Journal of Mechanical Design, 127(5), pp.931-940, September (2005)

[12] Soh G. S. and McCarthy J. M.: The synthesis of six-bar linkages as constrained planar 3R chains. Mechanism and Machine Theory, Volume 43, Issue 2, February 2008, pp.160-170

[13] McCarthy J. M. and Soh G. S.: Geometric Design of Linkages. Springer-Verlag, New York. (2010)

[14] Wampler C. W.: Solving the Kinematics of Planar Mechanisms by Dixon Determinant and a Complex Plane Formulation. ASME Journal of Mechanical Design, 123(3), pp.382-387, September (2001)

[15] Dixon, A. L.: The eliminant of three quantics in two independent variables. Proceedings of the London Mathematical Society. Volume 2, Number 1, pp. 49-69, 1909

[16] Nielsen J. and Roth B.: Solving the Input/Output Problem for Planar Mechanisms. ASME Journal of Mechanical Design, 121(2), pp.206-211, June (1999)

[17] Dhingra A. K., Almadi A. N., and Kohli D.: A Gröbner-Sylvester Hybrid Method for Closed-Form Displacement Analysis of Mechanisms. ASME Journal of Mechanical Design, 122(4), pp.431-438, December (2000)

[18] Porta J. M., Ros L., and Thomas F.: A Linear Relaxation Technique for the Position Analysis of Multiloop Linkages. IEEE Transactions on, 25(2), pp.225-239, April (2009)

[19] Chase T. R. and Mirth J. A.: Circuits and Branches of Single-Degree-of-Freedom Planar Linkages. ASME Journal of Mechanical Design, 115(2), pp.223-230, June (1993)

[20] Myszka D. H., Murray A. P., and Wampler C. W.: "Mechanism Branches, Turning Curves and Critical Points, *Proc. ASME 2012 Design Engineering Technical Conferences*, Paper No. DETC2012/70277, August 12-15, 2012, Chicago, IL, (2012)

[21] Kecskeméthy A., Krupp T., and Hiller M.: Symbolic processing of multiloop mechanism dynamics using closed-form kinematics solutions. Multibody System Dynamics 1(1), pp.23-45, March (1997)

[22] Whitney H.: Non-Separable and Planar Graphs. Transactions of the American Mathematical Society, Volume 34, No. 2, pp.339-362, April (1932)

[23] Dijkstra, E. W.: A note on two problems in connexion with graphs. Numerische mathematik, Volume 1, Number 1, pp. 269-271, 1959

[24] Silvester J. R.: Determinants of Block Matrices. The Mathematical Gazette, Volume 84, Issue 501, pp.460-467, November (2000)